Polymer Journal (2023) 55:1085–1095
https://doi.org/10.1038/s41428-023-00798-1

ORIGINAL ARTICLE

Printable Poly(*N*-acryloyl glycinamide) Nanocomposite Hydrogel Formulations

Nikola Majstorović[1] · Mohamed Zahedtalaban[1] · Seema Agarwal[1]

Received: 3 March 2023 / Revised: 4 May 2023 / Accepted: 9 May 2023 / Published online: 19 June 2023

Abstract

Printable synthetic polymer formulations leading to hydrogels with high strengths, swelling resistance, and bioactivities are required to control the mechanical and functional characteristics of biological scaffolds. Here, we present nanocomposite hydrogels prepared with the upper critical solution (UCST)-type polymer ink poly(*N*-acryloyl glycinamide) (PNAGA) and different concentrations of carbon nanotubes (CNTs). Nanofiller CNTs are recommended for increasing the bioactivities of hydrogel scaffolds. Printing methods were established in which the CNTs were included before and after the fabrication of the ink. The methods were compared to each other and their temperatures and shear-thinning properties were determined from the rheologies. A self-thickening method was utilized for 3D printing of nanocomposite constructs, and the printabilities varied with the CNT content and preparation method. After photopolymerization of the printed constructs, the nanocomposite hydrogel exhibited a slightly higher mechanical strength (15,500 Pa, $E_{mod} = 0.697 \pm 0.222$ MPa), great elasticity (elongation ~500%) and an electrical conductivity ($5.2{\cdot}10^{-4} \pm 1.5{\cdot}10^{-4}$ S·m^{-1}) comparable to that of the neat PNAGA hydrogel. Since high-strength constructs can be 3D printed with good resolution and low cytotoxicity, these nanocomposite hydrogel scaffolds could be used in biological and tissue engineering applications.

Introduction

Hydrogels are three-dimensional crosslinked polymer networks that swell in aqueous media [1, 2]. As they absorb and hold large quantities of water, they are interesting materials for various applications. For example, hydrogels are used in combination with hydrochars for water retention and nutrient release in agriculture [3]. In other applications, hydrogels are functionalized and used for wastewater treatment or in the pharmaceutical and food industries [4–7]. In biomedical applications, they mimic the extracellular matrix (ECM) and be used as scaffolds due to their softness and elasticities [2, 8, 9]. 3D bioprinting is a layer-by-layer assembly method that prints hierarchical scaffolds with high resolution and with tunable hydrogel-based bioinks. Ongoing research is conducted to satisfy the need for bioinks with good printabilities, biocompatibilities, and adequate mechanical stabilities [10, 11]. Other examples of 3D printed hydrogel materials include the stimuli-responsive actuators or solar evaporator gels used in applications such as regenerative biomedicine or desalination, respectively [12, 13]. These stimuli-responsive hydrogels change their volumes in response to external stimuli such as pH, ionic strength, or temperature [1, 14]. Among the known upper critical solution type (UCST) thermosensitive hydrogels, poly(*N*-acryloyl glycinamide) (PNAGA), which has a physically crosslinked polymer network, has received increasing attention in research on biological scaffolds. In addition to their thermosensitivities, PNAGA hydrogels exhibit high mechanical strengths, excellent elasticities, and anti-swelling properties stemming from hydrogen bonding of its dual-amide moieties [15, 16]. At low concentrations, PNAGA forms a soft, thermoreversible hydrogel with a sol-gel phase transition, while at high concentrations, high-strength, anti-swelling hydrogels are produced [16]. 3D printing of pure monomer inks is imprecise due to their low viscosities; therefore, filler materials or other viscosity-increasing methods can be used

Supplementary information The online version contains supplementary material available at https://doi.org/10.1038/s41428-023-00798-1.

✉ Seema Agarwal
agarwal@uni-bayreuth.de

[1] Macromolecular Chemistry II, Bavarian Polymer Institute, University of Bayreuth, Bayreuth 95440, Germany

with the inks. Xu et al. utilized the concentration-dependent hydrogen bonding-strengthening property of PNAGA to prepare a self-thickening PNAGA hydrogel as a meniscus substitute [17]. NAGA monomers and a photoinitiator were loaded into the highly viscous PNAGA hydrogels to create inks, and they could be thermally extruded from a nozzle due to the sol-gel transition. The printed gels were crosslinked under UV light to give high-strength constructs via formation of additional hydrogen bonds. In addition to the self-thickening strategy, tackifiers such as clay have been used to prepare viscous PNAGA nanocomposite inks used in 3D printing for bone regeneration. The clay increased the mechanical strengths of PNAGA hydrogels and enhanced cell interactions of the otherwise nonbioactive PNAGA at the same time [18]. Carbon nanotubes (CNTs) are widely used as nanofillers in nanocomposite hydrogels. They enhance the mechanical properties and add thermal and electrical conductivity to a hydrogel network [19]. Short multiwalled carbon nanotubes (MWCNTs) can be incorporated into a physically crosslinked hydrogel. Therefore, they are suitable for use with PNAGA inks and hydrogels. Nanocomposite hydrogels based on CNTs have shown increased stiffness and electrical conductivity, which is favorable for adhesion and proliferation of cells [20–22].

In this work, 3D-extrusion-printable PNAGA CNT nanocomposite inks were prepared. Two preparation methods were used in which the MWCNTs were added before and after the formation of the ink. The self-thickening inks were loaded into a 3D printer, and high-strength hydrogels were obtained after additional photopolymerization. The MWCNTs acted as a nanofiller to mechanically reinforce the physically crosslinked network and add bioactivity to the PNAGA hydrogel, as the cells tended to adhere to rigid surfaces. Owing to the self-thickening preparation method and the bioactivity-inducing CNTs, constructs with the PNAGA CNT nanocomposite hydrogels could be used to stimulate cell growth in bioapplications or to create scaffolds for tissue engineering via 3D printing.

Experimental

Materials

Glycinamide hydrochloride (98%, Biosynth Carbosynth, United Kingdom), acryloyl chloride (96%, Alfa Aesar), multiwalled nanotubes (MWNT) (Nanoamor Inc. (stock# 1237YJS, 95%, OD 20–30 nm, length 0.5–2 μm)), 2-hydroxy-4′-(2-hydroxyethoxy)-2-methylpropiophenone (IRGACURE-2959) (98%, Sigma Aldrich), potassium persulfate (KPS, 99%, Sigma Aldrich), *N,N,N′,N′*-tetramethylethylenediamine (TEMED) (≥ 99.0%, Sigma–Aldrich), sulfuric acid (95%, Merck), nitric acid (65%, Merck), and dialysis tubes (molecular weight cut off MWCO 12 ~ 14k, VWR International GmbH) were used as received. Milli-Q water was used for all experiments. Technical grade solvents were distilled prior to use. All other chemicals and solvents were analytical reagents. *N*-acryloyl glycinamide (NAGA) was prepared according to previous report [23].

Analytical measurements

The equilibrium swelling ratios (ESR) were determined by placing the washed PNAGA CNT nanocomposite hydrogels in polystyrene Petri dishes and swelling them in pure water at room temperature for 24 h. After removing the swelling medium, the hydrogels were blotted with filter paper and weighed (W_t). The gels were reswelled in pure water and weighed again after five days. The weighing process was repeated after two days and another three days. The hydrogels were then vacuum-dried (BINDER GmbH) at 40 °C for 24 h and weighed (W_d). The equilibrium swelling ratios (ESRs) of the gels were calculated as W_t/W_d. The mechanical strengths of the hydrogels were studied by viscoelastic rheological measurements on an Anton Paar MCR 203 rheometer using PP25 as a measuring system and a constant force of 0.5 N. Round gels were cut out with a 25 mm punching tool. Before the measurement, the linear viscoelastic range of the hydrogel was determined (LVE). Frequency sweep measurements were performed over the range 0.1–100 rad s^{-1}. The temperature-dependent viscosity changes of the PNAGA CNT inks were determined by rheology studies in the temperature range 30–90 °C. A cooling/heating cycle was applied with a cooling/heating rate of 5 °C min^{-1}. The frequency was 1 Hz, and the strain was 1%. Shear thinning was studied with a steady-state flow test at 80 °C and with shear rates of 1 to 1000 s^{-1}, and complex viscosity curves were obtained. Uniaxial mechanical tensile tests of the PNAGA CNT nanocomposite hydrogels were performed with a BT1-FR 0.5TND14 system (Zwick/Roell) at room temperature. The specimen samples were prepared by crosslinking a pregelled solution in a mold with the dimensions specified in DIN53504 S3. The thicknesses of the hydrogels were 2 mm. The hydrogels were stored at room temperature for 24 h and then measured with a test speed of 50 mm min^{-1}. The grip-to-grip separation was 20 mm. The elastic modulus was determined from the slope of the linear region of the stress-strain curve, and the tests were repeated at least three times. Thermogravimetric analyses (TGA) of the carbon nanotubes (CNTs) were performed with a TG 209 F1 Libra system (Netzsch). The samples were studied over the range 25–600 °C under nitrogen and synthetic air (O_2/N_2, 20/80, v/v) with a flow rate of 50 mL min^{-1}. Proteus Analysis

version 8.0 was used to analyze the data. The morphologies of the ox-MWCNTs were studied by elastic bright-field transmission electron microscopy (TEM) utilizing a JEOL JEM-2200FS EFTEM (JEOL GmbH, Freising, Germany) electron microscope operated at an acceleration voltage of 200 kV. A sample drop of an ox-MWCNT dispersion was trickled on a piece of carbon-coated copper grid. Before it was placed into the TEM specimen holder, the copper grid was air-dried under ambient conditions. Zero-loss filtered images were recorded with a Gatan CMOS (OneView) camera with GMS 3.11. The resistivity was measured with the four-point method. After the PNAGA CNT nanocomposite hydrogels were prepared, they were swelled in pure water for one week. The swelling medium was changed twice daily to remove ionic impurities. The distance between the electrodes was 1 mm. A Keithley 2401 SourceMeter was used as a source and measuring device. A current was applied through the electrodes, and a V-I graph was obtained. The resistance R was the slope of the linear region. The conductivity σ in $S\,m^{-1}$ was calculated as follows:

$$\sigma = \frac{d}{H \times W \times R} \quad (1)$$

where σ is the conductivity in $S{\cdot}m^{-1}$, d is the distance between electrodes, H is the sample thickness, and W is the sample width. The measurements were repeated at least three times, and the average was taken.

Oxidation of the multiwalled carbon nanotubes (ox-MWCNTs)

Oxidized MWCNTs (ox-MWCNTs) were prepared with a previously published procedure [24]. Briefly, 490 mg of multiwalled nanotubes (OD 20–30 nm, length 0.5–2 µm) were dispersed in 40 mL of a 3:1 solution of 95% H_2SO_4 and 65% HNO_3 (v/v) and sonicated for four hours at RT. After stirring for 24 h, the dispersion was purified with a dialysis tube (molecular weight cut off MWCO = 12–14 k) for seven days. The dispersion was frozen in liquid nitrogen and freeze-dried to obtain 395 mg of the ox-MWCNTs.

Preparation of self-thickening PNAGA CNT inks

Self-thickening PNAGA CNT inks were prepared with a modified literature procedure [17]. Two different formulations were prepared via Method 1 and Method 2.

In Method 1, a thermoreversible hydrogel with 4 wt% PNAGA was obtained by photopolymerizing a pregelled solution containing 300 mg of NAGA, 1.5 mg of potassium persulfate (0.5 wt% relative to NAGA) and 0.1 wt% CNTs (relative to NAGA) in 7488 µL of H_2O for 40 min. The gel was heated to 85 °C to become a sol. NAGA (3173 mg, 30 wt% relative to the gel mass) and IRGACURE-2959 (31.7 mg, 1 wt% relative to the gel mass) were added to the sol, and inks were obtained after cooling to RT. Inks with CNT contents of 0.25 wt% and 0.33 wt% were prepared analogously. As a control, an ink without any added CNTs was prepared likewise.

In Method 2, the thermoreversible hydrogel with 4 wt% PNAGA was prepared via photoinitiated polymerization with IRGACURE-2959 as the initiator and without added CNTs. After heating to 85 °C, the NAGA (30 wt% relative to the gel mass) and CNTs (0.1 wt% relative to the added NAGA) were dispersed in the sol and stirred for 10 min. After cooling to RT, the inks were obtained. The preparation was repeated analogously with 0.25 wt% and 0.33 wt% CNTs. As a control, an ink without added CNTs was prepared likewise.

The inks prepared were labeled Ink_x_y, where x denotes the preparation method used for formulation and y denotes the CNT content in wt% relative to NAGA.

Preparation of a self-thickening PNAGA CNT nanocomposite hydrogel

PNAGA CNT nanocomposite hydrogels were prepared by heating the inks from Method 1 or Method 2 to their sol state at 85 °C; they were transferred into round Teflon molds (diameter of 2.5 cm and thickness of 1 mm), and covered with glass slides. The photocrosslinking reaction was conducted at RT and with irradiation by a UVAHAND lamp for 10 min. The gels were stored in pure water at room temperature, and the swelling medium was replaced daily for two days. The hydrogels were labeled Gel_x_y, where x denotes the method used for the gel preparation and y denotes the CNT content in wt% relative to NAGA (e.g., Gel_2nd_0.33).

3D printing of the self-thickening PNAGA CNT nanocomposite hydrogels

The PNAGA CNT inks were transferred to alumina cartridges (Cellink) and placed in the printhead of a pneumatic bioprinter Inkredible+ (Cellink). The gauge of the needle was 24 G. The inks were tempered at different printing temperatures for 8 min before printing. A pressure of 60 kPa was applied. G-code was generated with the software Heartware (Cellink). The feed rate was specific to the printer and included in the G-code generated by the software.

Live/Dead viability assay

The hydrogel discs were preincubated in 24-well plates with complete cell culture medium (HBSS) for 24 h. Then,

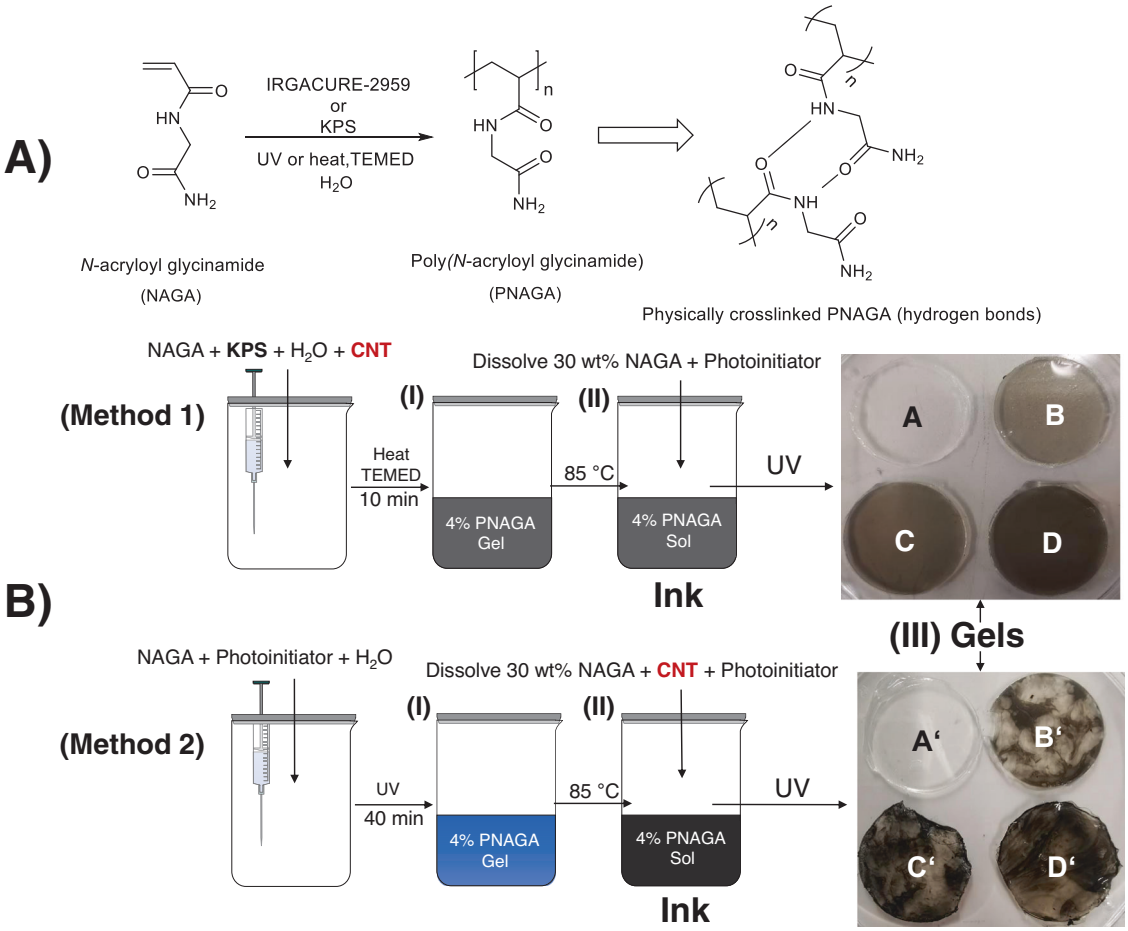

Scheme 1 **A** Free-radical polymerization of NAGA into PNAGA with initiators such as potassium persulfate (KPS) or the photoinitiator IRGACURE-2959. The polymer PNAGA formed hydrogen bonds in aqueous solution. **B** Preparation of PNAGA CNT inks and gels. In preparation Method 1, appropriate amounts of monomeric NAGA, KPS, and CNTs were polymerized into a soft and thermoreversible hydrogel by heating with the accelerator TEMED (4 wt%, Step I). Then, the gel was heated to 85 °C and loaded with 30 wt% additional NAGA monomer and photoinitiator (Step II). In Method 2, 4 wt% NAGA was photopolymerized into a soft and thermoreversible hydrogel (4 wt%, Step I). It was heated to 85 °C and loaded with 30 wt % added NAGA monomer, photoinitiator, and CNT to obtain the ink (Step II). After cooling, both inks were subjected to further UV photopolymerization to yield the PNAGA CNT hydrogels (Step III, A – D and A' – D', respectively)

L929 cells were incubated on the hydrogel discs for 96 h (0.05×10^6 cells/well). After that, they were stained with 200 µL of dye/well (Live/Dead dye, Reduced Biohazard Kit, Thermo Fisher Scientific) for one hour. The staining solution was removed, and discs in the wells were washed four times with 200 µL HBSS/well. Then, the cells were fixed with 4% glutaraldehyde in HBSS for three hours at RT. After removal of the fixative, the discs were washed once with HBSS and stored at 4 °C in HBSS (250 µL/well).

He stained cells were examined with a Leica DMR fluorescence microscope. An excitation filter cube with a wavelength range of 450–490 nm, a dichromatic mirror of 510 nm, and a suppression filter of LP 515 nm distinguished the live cells (green) and dead cells (red) in the microscope image. The images were visualized with Image Capture and Leica QWin software.

Statistical analyses

The hydrogel equilibrium swelling experiments, tensile tests, and rheological experiments were performed at least three times unless otherwise stated. The means and standard deviations are given.

Results and discussion

Preparation of self-thickening PNAGA CNT nanocomposite hydrogels

Before preparation of the self-thickening poly(*N*-acryloyl glycinamide) carbon nanotube (PNAGA CNT) nanocomposite hydrogels, the multiwalled carbon nanotubes (MWCNTs) were modified into a more soluble form to

ensure homogenous dispersion of the CNTs in the pregel solution. The solubility of the carbon nanotubes was increased by oxidizing them in a highly acidic environment (ox-MWCNT) (Fig. S1a). The resulting carboxylate functionalities on the CNT surface allowed enhanced dispersion in aqueous solutions. The successful oxidation of the MWCNTs and their characterization data are explained in Fig. S1A–D. Briefly, the CNTs were ultrasonicated in a mixture of H_2SO_4 and HNO_3 for several hours to introduce these hydrophilic carboxyl groups. The modified CNTs showed different thermal degradation and dispersion behaviors in water. In the PNAGA CNT nanocomposite formulations, the CNT concentrations were kept deliberately low to avoid incomplete conversion to the hydrogel, as the CNTs could absorb the UV light needed for the crosslinking reaction.

Self-thickening PNAGA hydrogels were prepared by first photopolymerizing a low-concentration pregel solution with 4 wt% NAGA and forming a soft PNAGA hydrogel with a sol-gel phase transition. The free-radical polymerization of NAGA into the PNAGA hydrogel is depicted in Scheme 1.

The preparation of the self-thickening PNAGA CNT nanocomposite hydrogels is depicted in Scheme 1. As shown, 30 wt% of NAGA monomer was loaded (loading step) into the thermoreversible gel to obtain the printable inks. The concentrations used in preparing the inks were chosen according to a previously established formulation [17]. Depending on whether the CNTs were added to the pregel solution or during the loading step, two different preparation methods, Method 1 and Method 2, respectively, were developed. In Method 1, a low-strength, thermoreversible PNAGA hydrogel was prepared by thermal polymerization of the NAGA monomer by using potassium persulfate (KPS) as the initiator in the presence of the CNTs. Prolonged ultrasonication was used to ensure homogenous dispersion of the CNTs in solution. Since the CNTs absorb light, photoinitiators were not chosen because conversion into soft hydrogels would be inefficient [25]. Upon heating to a temperature of 85 °C, the gel became a sol; NAGA and the photoinitiator were added in the next step to obtain an ink. The inks could be reshaped into discs. Since they were thin, sufficient long-wavelength UV crosslinking yielded the PNAGA CNT nanocomposite hydrogels (Scheme 1A–D). With increasing CNT concentration, the discs became darker. In Method 2, the CNTs were added in the loading step after photocrosslinking of the soft PNAGA hydrogels. Since no CNTs were added to the pregel solution, photopolymerization was performed instead of thermal polymerization, and this resulted in high conversion rates. While the thermoreversible gel became a sol at high temperature, the CNTs were added, and the mixture was stirred and ultrasonicated. However, in contrast to Method 1, the CNTs were not adequately homogenized throughout the sol. After the UV treatment, discs were obtained in which domains with different CNT concentrations were visible (Scheme 1A'–4D'). The disc thicknesses also decreased with increasing CNT concentration, since a higher concentration led to partial absorption of the UV light needed for polymerization. This led to bending or rolling of the hydrogel discs, as they were not stable in a planar state. It should be noted that the concentration of CNTs in Method 1 was relative to the NAGA monomer concentration in the pregel solution (4 wt% NAGA), while in Method 2, the concentration of CNTs was relative to the NAGA monomer added during the loading step (30 wt% NAGA). Therefore, the total concentration of CNTs in the Method 1-derived gels was lower than that in the Method 2-derived hydrogels. As higher CNT concentrations absorb more of the UV light required for photocrosslinking polymerization, the Method 2-type hydrogels exhibited less efficient conversion into fully crosslinked hydrogels than the Method 1-type hydrogels.

Characterization of the PNAGA CNT inks

For a proper 3D printing setup exhibiting smooth printing, the viscosities of the inks were studied as a function of the temperature or shear rate. In this work, CNTs with different concentrations from 0 to 0.33 wt% relative to the NAGA monomer were included in the ink mixture. As the inks were used for extrusion-based 3D printing, the temperature-dependent rheological properties of the unloaded PNAGA hydrogel and the loaded ink were studied for both preparation methods (Fig. S2). When no CNT or additional NAGA monomer were added, the neat soft 4 wt% PNAGA hydrogel passed into the sol state at approximately 85 °C (Figs. S2A and S3A). When the CNTs were used in the first preparation step of the 4 wt% PNAGA gel, the sol-gel phase transition was shifted to higher temperatures for the Method 1-type inks (85–92 °C) (Fig. S2B–D, Step I in Scheme 1). The CNTs provided mechanical reinforcement of the polymer matrix, which required a higher temperature to break the hydrogen bonds formed in the physically crosslinked hydrogel [26]. On the other hand, the intermolecular interactions were disturbed by adding the NAGA monomer. The ink exhibited a lower phase transition temperature and weaker mechanical strength (Fig. S2E–G). For printability, a lower phase transition temperature is desirable, so the printing parameters were fine-tuned by changing the concentration of the CNTs.

In Method 2-type inks, the CNTs were added during the NAGA loading step. The viscosity changes occurring in the thermoreversible PNAGA hydrogels at various temperatures were compared before and after loading (Fig. S3B–D). In Method 2, a photoinitiator was used to prepare the gels,

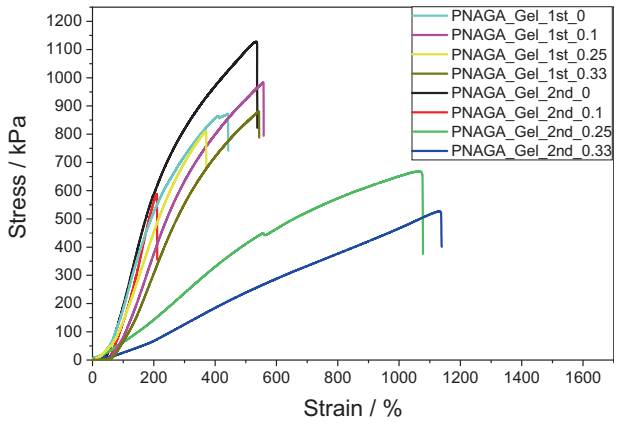

Fig. 1 Stress–strain curves for the PNAGA CNT nanocomposite hydrogels

while the Method 1-type inks were prepared via redox polymerization with KPS. The sol-gel phase transition temperature of the latter was higher, possibly due to the gentler reaction conditions that preserved the hydrogen bonds constructed between the chains. Upon adding the monomer, the phase transition temperature was lowered. As with the Method 1-type inks, the NAGA monomer disturbed the hydrogen bonding of the gel, which resulted in a lower phase transition temperature. The effects of CNTs in the gel were not observed, as a similar drop in phase transition temperature was found regardless of the CNT concentration.

Steady-state flow experiments were performed with the PNAGA CNT inks to study the dynamic viscosities for different shear rates at 80 °C (Fig. S4). It is known that PNAGA hydrogels exhibit shear-thinning [16, 17]. A temperature of 80 °C was chosen because the inks were near the sol-gel phase transition (Figs. S2 and S3). The viscosities of the studied inks decreased gradually with increasing shear rates. At 1 s^{-1}, the soft 4 wt% PNAGA hydrogel without CNTs or added NAGA had the lowest starting viscosity (Methods 1 and 2, Fig. S4, black). With increasing shear rates, the viscosity dropped to the lowest value among the inks studied here. Adding the NAGA monomer to the 4 wt % PNAGA hydrogel (Methods 1 and 2) increased the viscosity relative to that for the unloaded PNAGA when continuous shearing was applied. When the CNTs were added together with the NAGA monomer, the PNAGA CNT inks showed slightly weaker shear-thinning than the loaded neat PNAGA hydrogel (Method 2, Fig. S4, red, green, blue, turquoise). Therefore, the CNT content in the ink influenced the shear-thinning properties to some degree. It is assumed that shear-thinning would be further reduced if inks with higher CNT contents were subjected to shearing forces. Overall, the CNTs had a positive influence on the temperature-dependent viscosity changes by reinforcing the polymer network structure, while in the steady-state flow experiments, the CNTs only slightly lowered the shear thinning capacities of the inks.

Mechanical characterization of the PNAGA CNT Hydrogels

The mechanical toughnesses of the PNAGA CNT hydrogels were studied with frequency sweep experiments (Figs. S5 and S6). The storage moduli of the Method 1-type hydrogels differed slightly from that of the non-CNT PNAGA. The hydrogels made with low CNT concentrations exhibited storage moduli of ~7000 Pa, as shown in Fig. S5B, C, which was lower than that of the neat PNAGA hydrogel (G' ~ 12,500 Pa). However, the highly concentrated CNT hydrogel exhibited a storage modulus of approximately 15,500 Pa. (Fig. S5D). As discussed, the CNTs increased the gel stiffness when incorporated into the network [20, 27]. A higher concentration of CNTs would strengthen the hydrogel network even more, but a lower conversion would result for the UV crosslinking reactions, so a CNT concentration of 0.33 wt% was chosen as the threshold.

In the Method 2-type hydrogels, the CNTs were added together with the monomers to the 4 wt% PNAGA hydrogels during the loading step. Because of the high viscosity, it was challenging to integrate the CNTs into the gel matrix by mixing. As a result, the CNTs were heterogeneously dispersed in the ink [28]. After thickening of the ink, the mechanical stiffness was studied with rheological experiments (Fig. S6). The added CNTs barely changed the mechanical characteristics of the Method 2-type hydrogels. A storage modulus of approximately 4000 Pa at a frequency of 1 s^{-1} was reported for the hydrogels. As mentioned before, the difficulty in dispersing the CNTs in the viscous matrix was attributed to the formation of CNT aggregates. In this case, the network did not fully utilize the mechanical strengthening capability of the CNTs. However, Gel_2nd_0.33, which exhibited the highest CNT concentration in the studied series, had a marginally higher storage modulus of 4500 Pa. As explained for Method 1, the CNTs reinforced the mechanical stiffness, and theoretically, a higher CNT concentration would increase the hydrogel rigidity even more.

Physically crosslinked PNAGA has excellent elasticity due to its flexible hydrogen bonding interactions. Consequently, PNAGA CNT hydrogels should perform similarly when stretched. Figure 1 shows the stress–strain curves for various PNAGA CNT hydrogels prepared with both Methods 1 and 2.

Neat PNAGA was prepared without any CNT content via preparation Method 1 and had an elongation at break and elastic modulus E_{mod} (442.0 ± 96.7% and 0.277 ± 0.084 MPa) similar to those of the Method 2-type samples (533.8 ± 125.2% and 0.327 ± 0.068 MPa). In

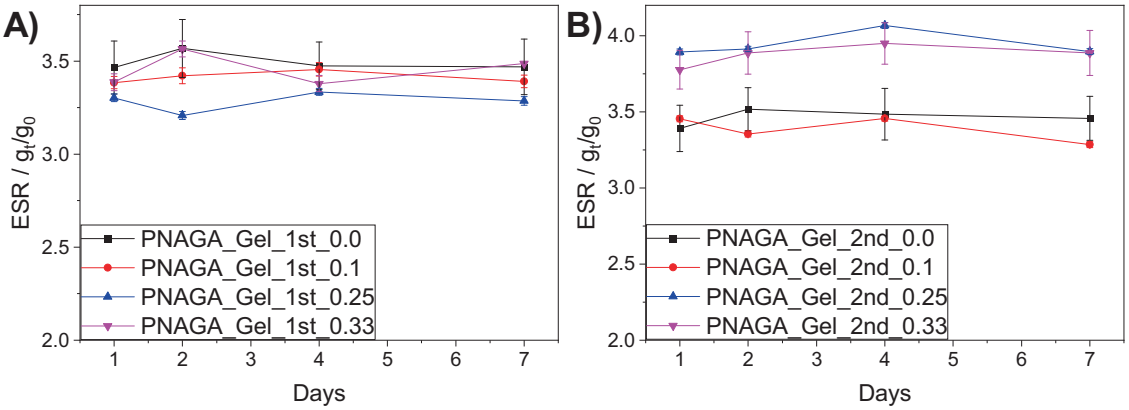

Fig. 2 Equilibrium swelling ratios of (**A**) the Method 1-type hydrogels and (**B**) the Method 2-type hydrogels

Method 1, the ink was prepared by thermal polymerization initiated with KPS, while in Method 2 the inks were prepared by photoinitiation. Furthermore, the difference between the two methods was the different polymerization times. As the polymerization was catalyzed with the accelerator TEMED, the gel in Method 1 was formed after a short polymerization time. For photopolymerization Method 2, a much longer polymerization time with exposure to UV light was employed for conversion into the hydrogel, which might have resulted in slightly different mechanical strengths and elasticities.

The elongation at break for the Method 1-type hydrogel was approximately 500%, similar to that for the neat PNAGA hydrogel. The CNT concentration affected the elastic modulus in Gel_1st_0.33 by reinforcing the hydrogel network. Here, a considerably high E_{mod} of 0.697 ± 0.222 MPa was reported. The change in mechanical strength resulting from mechanical reinforcement by the CNTs was evident for the Method 1-type hydrogels. Among the Method 2-type hydrogels, Gel_2nd_0.1 had the shortest elongation at break, $409.6 \pm 2.1\%$. However, the elongations at break for Gel_2nd_0.25 and 0.33 were noticeably high at $1428.1 \pm 453.8\%$ and $1532.8 \pm 338.4\%$, respectively. Since they had the highest amounts of CNTs added to the ink, the CNTs absorbed a significant amount of UV light required for the complete conversion of the ink into the hydrogel. The hydrogels were thin, and the low crosslinking conversion led to highly elastic hydrogels with low E_{mod} values (0.031 ± 0.002 MPa and 0.021 ± 0.007 MPa, respectively).

Equilibrium swelling studies

Swelling of the different PNAGA CNT hydrogels was studied gravimetrically over seven days (Fig. 2). The equilibrium swelling ratios (ESRs) of the gels remained similar at approximately 3.4 to 4, even after addition of the CNTs. The ESRs of the Method 1-type hydrogels barely differed from each other. The effects of the CNTs on swelling of the polymer network were negligible due to the low concentration of CNTs dispersed in the hydrogel. In the Method 2-type hydrogels, the equilibrium swelling ratios were slightly higher for hydrogels with higher CNT contents, such as Gel_2nd_0.25 and Gel_2nd_0.33. As discussed earlier, the high CNT content absorbed the UV light needed for complete conversion into the hydrogel. A lower conversion was accompanied by a lower crosslinking degree, which resulted in greater swelling [29]. The ESRs of the hydrogels remained constant for seven days, demonstrating the anti-swelling properties already reported for self-thickening, non-CNT PNAGA [17]. For 3D printing and tissue engineering purposes, the limited swelling of gels was particularly important for preparing constructs that remained stable in shape and size.

Conductivity experiments

The CNT-enhanced hydrogels were shown to have conductivities essential for cell compatibility [28, 30]. In this work, the conductivities of the PNAGA CNT hydrogels were calculated from resistivity measurements. The conductivities of the Method 1-type hydrogels increased with increasing CNT concentration, as shown in Fig. 3A. The non-CNT PNAGA hydrogel had a conductivity of $1.5 \cdot 10^{-4} \pm 2.9 \cdot 10^{-5}$ S·m^{-1}, which was attributed to residual acrylate groups or dissolved CO_2. Gel_2nd_0.33 had the highest CNT concentration and, therefore, the highest conductivity of $4.1 \cdot 10^{-4} \pm 9.8 \cdot 10^{-5}$ S·m^{-1}.

In the Method 2-type hydrogels, the conductivities increased gradually from the lowest value of $2.2 \cdot 10^{-4} \pm 1.9 \cdot 10^{-5}$ S·m^{-1} for neat PNAGA to the highest value of $5.2 \cdot 10^{-4} \pm 1.5 \cdot 10^{-4}$ S·m^{-1} for Gel_2nd_0.25 (Fig. 3B). Curiously, the Gel_2nd_0.33 hydrogel with the high CNT concentration had a comparatively low conductivity of $2.3 \cdot 10^{-4} \pm 5.7 \cdot 10^{-5}$ S·m^{-1}. Since carbon nanotubes form aggregates when dispersed in highly viscous polymer mixtures, as was the case for the Method 2-type inks, the heterogeneously dispersed CNTs

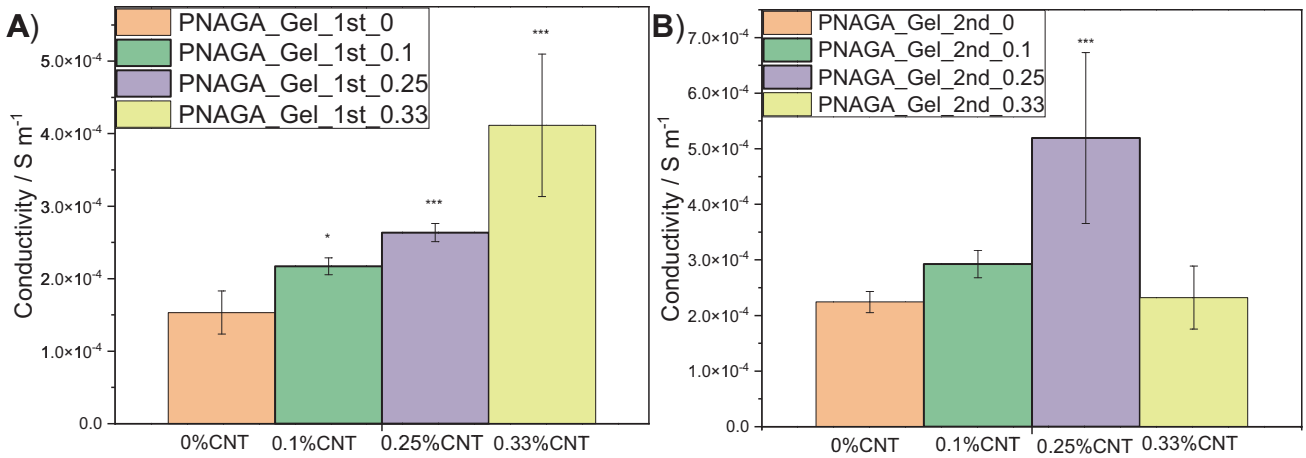

Fig. 3 Electrical conductivities of the PNAGA CNT nanocomposite hydrogels. (**A**) Method 1-type gels (**B**) Method 2-type gels. $*p < 0.05$ and $***p < 0.001$ compared to the 0% CNT PNAGA hydrogel (one-way ANOVA, Dunn-Sidak test)

generated anisotropic conductivities [28]. It was expected that conductivity would not increase linearly with the CNT content due to aggregation. Instead, the conductivity may drop when the CNTs aggregated in the ink mixture, which is likely with a sufficiently high CNT concentration.

Extrusion-based 3D printing of the PNAGA CNT nanocomposite hydrogels

Due to their thermoreversibilities and shear-thinning properties, the PNAGA CNT inks should be viable for 3D printing. The shape fidelity, homogeneity, and strength of the printed construct can be fine-tuned with parameters such as the printing temperature, pressure, nozzle size, and feed rate. In preliminary experiments, 4 wt% PNAGA hydrogels without monomer, CNT, or initiator were printed with different parameters (Fig. S7). As indicated by the rheological studies, the unloaded hydrogel had a high sol-gel phase transition temperature because loading with monomeric NAGA weakened the intermolecular hydrogen bonds supporting the gel network. Therefore, different printing parameters were expected for successful printing with the unloaded and loaded hydrogels. Due to their soft natures and moderate shear thinning properties, printing was difficult with the unloaded PNAGA gels. From A–D, the printing pressure was gradually reduced from 300 to 150 kPa. At higher pressures, the shape fidelity and homogeneity of the construct were insufficient, and the line thickness was very substantial (Fig. S7A). Upon decreasing the pressure, finer lines were obtained. At these low pressures, higher temperatures of 63 to 65 °C were necessary; otherwise, the sol-gel transition temperature of the gel was not reached during continuous printing. Overall, with a pressure of 150 kPa and printhead temperature of 65 °C, a thin construct exhibiting moderately good shape fidelity and structural integrity was obtained (Fig. S7D).

After loading the soft 4 wt% PNAGA with NAGA monomer into the inks, a different printing behavior was observed (Fig. S8). A drastic improvement was observed in the shape fidelity and homogeneity of gel printing. The added NAGA monomer influenced the hydrogen bonding in the gel network, as shown in the rheological experiments. Usually, NAGA interacts with the hydrogen bonds formed in soft hydrogels, weakens them and lowers the sol-gel transition temperature. The inks were tempered at higher temperatures than those used with the nonloaded inks. At a temperature of 75 °C, a construct was printed with good shape fidelity, thinner lines, and continuous printing without interruption. To be exact, loading the monomer into the ink lowered the phase transition temperature. With a moderate pressure of 200 Pa, favorable conditions for printing the loaded inks were realized (Table S2).

In the final 3D printing experiment, the printing inks made with Methods 1 and 2 were studied (Fig. 4, Table 1). The addition of CNTs during or after preparation of the thermoreversible hydrogels (Methods 1 and 2, respectively) altered the printabilities and appearances of the photo-crosslinked structures. As discussed above, the CNTs were not homogenously distributed in the Method 2-type hydrogels (Fig. 5C, D). While the gel became a fluid at high temperatures, the CNTs were barely dispersed in the gel matrix, which resulted in an inhomogeneous distribution of the CNTs even after crosslinking. In the Method 1-type inks, the CNTs were more dispersed because they were added prior to the crosslinking reaction of the thermoreversible hydrogel ink. More homogenous printed structures were obtained (Fig. 4A, C).

Increased shape fidelity and structural integrity were observed in printing with the CNT-containing inks compared to previous printing attempts without the CNTs. The CNTs reinforced the hydrogen bonds, increased the mechanical strength of the PNAGA hydrogel network and

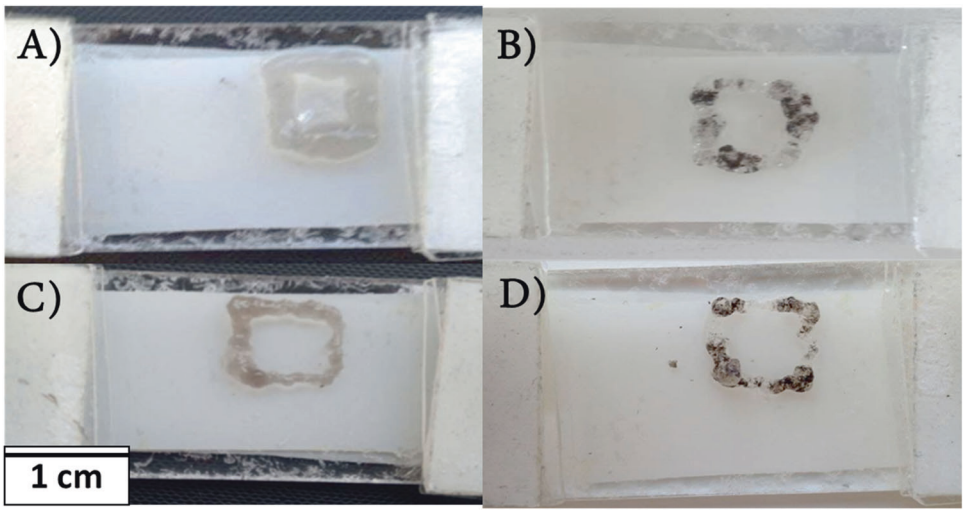

Fig. 4 3D structures printed with the PNAGA CNT nanocomposite hydrogels; **A**, **C** Gel_1st_0.1. **B**, **D** Gel_2nd_0.1

Table 1 Parameters used for 3D printing the constructs A–D in Fig. 4

Parameter	A	B	C	D
Pressure/kPa	200	150	**150**	180
Temperature/°C	75	70	**70**	75
Feed rate	250	200	**200**	200
Line thickness/cm	0.271	0.217	**0.172**	0.256

The bold parameters were found to be the most suitable for printing

enabled smoother printing. A printing pressure of 150 kPa, a temperature of 70 °C, and a feed rate of 200 enabled the printing of fine lines. However, the printing parameters could be further optimized to increase the homogeneity and enable printing of more complex 3D structures.

Live/dead cell viability assay

After incorporating CNTs into the hydrogel network, the cytocompatibilities of the PNAGA CNT hydrogels was studied with live/dead cell viability assays. L929 cells were seeded onto the hydrogels for 48 h. The live cells were stained with SYTO 10, a green fluorescent nucleic acid dye, and the dead cells were stained with DEAD Red, a red fluorescent nucleic acid dye. The cells on the Method 1-type hydrogels were viewed under a fluorescence microscope, and the resulting images are shown in Fig. 5.

Live or dead cells were barely observed as clusters on the neat PNAGA hydrogel without CNT incorporation, as only single live cells were found on the hydrogel. With increasing CNT concentration, larger clusters of the live cells were observed. In particular, Gel_1st_0.33 had several clusters of live cells (Fig. 5D). Since the CNTs increase biocompatibility by reinforcing the mechanical strength and electrical conductivity of a gel, more cells should have grown on the hydrogel. A similar observation was made for the Method 2-type hydrogels (Fig. S9). The non-CNT PNAGA hydrogel showed singular cells, but large clusters were found only in the PNAGA CNT hydrogels. In the Gel_2nd_0.33 hydrogels, single dead cells (red) were seen, but green live cell clusters were predominant. Overall, the PNAGA CNT hydrogels showed good cytocompatibilities with different CNT concentrations. Cytometric methods should be deployed to understand the cell behavior in the hydrogels.

Conclusion

Physically crosslinked nanocomposite hydrogels based on PNAGA and CNTs were successfully prepared via two distinct methods. The self-thickening property of the PNAGA was utilized when the thermoreversible low-concentration PNAGA was combined with monomeric NAGA and CNTs to form printable inks. Depending on when CNTs were added during the preparation procedure, the inks showed varying homogeneities for the CNTs inside the gel matrixes. The sol-gel phase transition temperature could be fine-tuned with the addition of CNTs, as shown for the inks with greater homogeneous CNT dispersion. The shear-thinning properties increased with increasing CNT concentrations, which facilitated modification of the printability of the PNAGA CNT inks. The mechanical properties of the PNAGA CNT hydrogels were studied with tensile tests and rheological methods, and it was found that CNTs reinforced the stiffness of the hydrogel network, and elongation depended on the conversion of the ink into the hydrogel. The 3D printing resolution depended on the homogeneity of the CNT dispersion in the inks, and suitable printability was achieved with moderate pressures and temperatures. The CNT-containing printed hydrogels showed greater shape fidelity and structural integrity than the non-CNT PNAGA hydrogels. Cell viability studies showed that the PNAGA CNT nanocomposite hydrogels supported the growth of larger cell

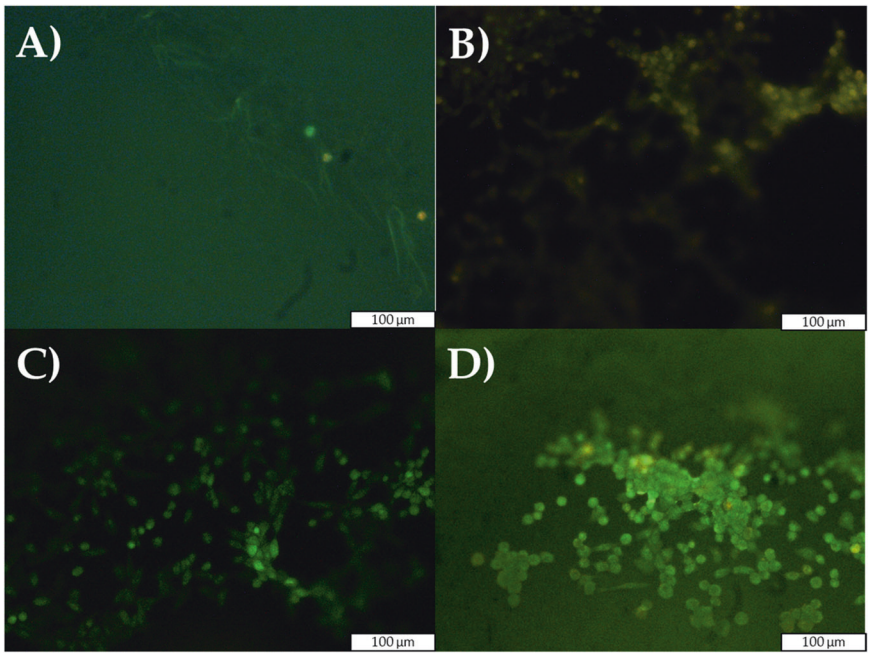

Fig. 5 Live/dead staining of the PNAGA CNT nanocomposite hydrogels prepared with Method 1; **A** Gel_1st_0, **B** Gel_1st_0.1, **C** Gel_1st_0.25, **D** Gel_1st_0.33

clusters. The cytotoxicity was low, as only single dead cells were found at higher CNT concentrations. The cell viabilities of these PNAGA CNT nanocomposite hydrogels should be studied further to determine the suitability of the PNAGA CNT hydrogels for cell growth. The printing parameters could be fine-tuned to print complex structures for tissue engineering or other bioapplications.

Acknowledgements We thank Dr. Valérie Jérôme for carrying out the cell viability tests. Electron and Optical Microscopy KeyLabs of Bavarian Polymer Institute is acknowledged for the facilities provided for scanning and transmission electron microscopy.

Funding Open Access funding enabled and organized by Projekt DEAL.

Compliance with ethical standards

Conflict of interest The authors declare no competing interests.

Publisher's note Springer Nature remains neutral with regard to jurisdictional claims in published maps and institutional affiliations.

References

1. Ahmed EM. Hydrogel: Preparation, characterization, and applications: A review. J Adv Res. 2015;6:105–21.
2. Slaughter BV, Khurshid SS, Fisher OZ, Khademhosseini A, Peppas NA. Hydrogels in regenerative medicine. Adv Mater. 2009;21:3307–29.
3. Zhang Y, Tian X, Zhang Q, Xie H, Wang B, Feng Y. Hydrochar-embedded carboxymethyl cellulose-g-poly (acrylic acid) hydrogel as stable soil water retention and nutrient release agent for plant growth. Hydrochar-embedded carboxymethyl Cellul-g-poly (acrylic acid) hydrogel stable soil water Retent nutrient release agent plant growth 2022;7:116–27.
4. Van Tran V, Park D, Lee Y-C. Hydrogel applications for adsorption of contaminants in water and wastewater treatment. Hydrogel Appl adsorption Contam water wastewater Treat. 2018;25:24569–99.
5. Szekalska M, Puciłowska A, Szymańska E, Ciosek P, Winnicka K. Alginate: Current use and future perspectives in pharmaceutical and biomedical applications. Alginate: Curr Use Future Perspect Pharm Biomed Appl. 2016;2016:7697031.
6. Aida TM, Kumagai Y, Smith RL. Mechanism of selective hydrolysis of alginates under hydrothermal conditions. Mechanism selective Hydrolys alginates hydrotherm Cond. 2022;7:173–9.
7. Li J, Jia X, Yin L. Hydrogel: Diversity of structures and applications in food science. Hydrogel: Diversity Struct Appl Food Sci. 2021;37:313–72.
8. Annabi N, Tamayol A, Uquillas JA, Akbari M, Bertassoni LE, Cha C, et al. 25th anniversary article: Rational design and applications of hydrogels in regenerative medicine. Ad Mater. 2014;26:85–123.
9. Van Vlierberghe S, Dubruel P, Schacht E. Biopolymer-based hydrogels as scaffolds for tissue engineering applications: a review. Biomacromolecules 2011;12:1387–408.
10. Schwab A, Levato R, D'Este M, Piluso S, Eglin D, Malda J. Printability and shape fidelity of bioinks in 3D bioprinting. Chem Rev. 2020;120:11028–55.
11. Gao F, Ruan C, Liu W. High-strength hydrogel-based bioinks. Mater Chem Front. 2019;3:1736–46.

12. Zhang A, Wang F, Chen L, Wei X, Xue M, Yang F, et al. 3D printing hydrogels for actuators: A review. 3D Print hydrogels Actuators: A Rev. 2021;32:2923–32.
13. Zheng X, Bao Y, Huang A, Qin G, He M. 3D printing double-layer hydrogel evaporator with surface structures for efficient solar steam generation. 3D Print double-layer hydrogel evaporator Surf Struct Effic Sol steam Gener. 2023;306:122741.
14. Pinelli F, Magagnin L, Rossi F. Progress in hydrogels for sensing applications: a review. Mater Today Chem. 2020;17:100317.
15. Dai X, Zhang Y, Gao L, Bai T, Wang W, Cui Y, et al. A Mechanically Strong, Highly Stable, Thermoplastic, and Self-Healable Supramolecular Polymer Hydrogel. Adv Mat. 2015;27:3566–71.
16. Xu Z, Liu W. Poly(N-acryloyl glycinamide): A fascinating polymer that exhibits a range of properties from UCST to high-strength hydrogels. Chem Commun. 2018;54:10540–53.
17. Xu Z, Fan C, Zhang Q, Liu Y, Cui C, Liu B, et al. A self-thickening and self-strengthening strategy for 3D printing high-strength and antiswelling supramolecular polymer hydrogels as meniscus substitutes. Adv Funct Mater. 2021;31:2100462.
18. Zhai X, Ma Y, Hou C, Gao F, Zhang Y, Ruan C, et al. 3D-Printed high strength bioactive supramolecular polymer/Clay Nanocomposite hydrogel scaffold for bone regeneration. ACS Biomater Sci Eng. 2017;3:1109–18.
19. Du JH. The present status and key problems of carbon nanotube based polymer composites. Express Polym Lett. 2007;1:253–73.
20. Ravanbakhsh H, Bao G, Latifi N, Mongeau LG. Carbon nanotube composite hydrogels for vocal fold tissue engineering: Biocompatibility, rheology, and porosity. Mater Sci Eng C. 2019;103:109861.
21. Vashist A, Kaushik A, Vashist A, Sagar V, Ghosal A, Gupta YK, et al. Advances in Carbon Nanotubes-Hydrogel Hybrids in Nanomedicine for Therapeutics. Adv Healthc Mater. 2018;7:e1701213–e1701213.
22. Gonçalves EM, Oliveira FJ, Silva RF, Neto MA, Fernandes MH, Amaral M, et al. Three-dimensional printed PCL-hydroxyapatite scaffolds filled with CNTs for bone cell growth stimulation. J Biomed Mater Res - B Appl. 2016;104:1210–9.
23. Seuring J, Bayer FM, Huber K, Agarwal S. Upper Critical Solution Temperature of Poly(N-acryloyl glycinamide) in Water: A Concealed Property. Macromolecules 2012;45:374–84.
24. Pistone A, Ferlazzo A, Lanza M, Milone C, Iannazzo D, Piperno A, et al. Morphological modification of MWCNT functionalized with HNO3/H2SO4 mixtures. J Nanosci Nanotechnol. 2012;12:5054–60.
25. Gallastegui A, Dominguez-Alfaro A, Lezama L, Alegret N, Prato M, Gómez ML, et al. Fast Visible-light photopolymerization in the presence of multiwalled carbon nanotubes: Toward 3D printing conducting nanocomposites. ACS Macro Lett. 2022;11:303–9.
26. Ghoshal S. Polymer/Carbon Nanotubes (CNT) Nanocomposites Processing Using Additive Manufacturing (Three-Dimensional Printing) Technique: An Overview. Fibers. 2017;5:40.
27. Mihajlovic M, Mihajlovic M, Dankers PYW, Masereeuw R, Sijbesma RP. Carbon nanotube reinforced supramolecular hydrogels for bioapplications. Macromol Biosci. 2019;19:1800173.
28. Liu X, Miller IiAL, Park S, Waletzki BE, Terzic A, Yaszemski MJ, et al. Covalent crosslinking of graphene oxide and carbon nanotube into hydrogels enhances nerve cell responses. J Mater Chem. B 2016;4:6930–41.
29. Dave PN, Gor A Chapter 3 - Natural Polysaccharide-Based Hydrogels and Nanomaterials: Recent Trends and Their Applications. In: Mustansar Hussain C, editors. Handbook of Nanomaterials for Industrial Applications: Elsevier, 2018, p. 36–66.
30. Shah K, Vasileva D, Karadaghy A, Zustiak SP. Development and characterization of polyethylene glycol–carbon nanotube hydrogel composite. J Mater Chem. B 2015;3:7950–62.